Time–Frequency Synchronization in Filtered Multitone Modulation Based Systems

Antonio Assalini
Dept. of Information Engineering – DEI
Padova, Italy
e–mail: assa@dei.unipd.it

Andrea M. Tonello
Dept. of Electrical Engineering – DIEGM
Udine, Italy
e–mail: tonello@diegm.uniud.it

***Abstract*— In this paper[§] we consider the problem of acquiring time and frequency synchronization in a filtered multitone (FMT) modulated system. An FMT based system differs from the popular OFDM system in the deployment of sub–channel shaping filters. Although the synchronization problem in OFDM is well understood, in an FMT system it presents several challenges. A number of techniques for the offsets correction are proposed. The transmission filter bank proprieties are exploited in the time domain before the demodulator. The use of special training symbol is also discussed.**

***Index Terms*— Filtered multitone modulation, OFDM, time–frequency synchronization.**

I. Introduction

Multicarrier modulation has attracted great attention for application to wideband wireless channels. This is because it has the potentiality of simplifying the equalization task that becomes mandatory in wideband channels experiencing severe frequency selectivity. Orthogonal frequency division multiplexing (OFDM) is probably among the most popular multicarrier modulation techniques. More general multicarrier schemes deploy sub–channel filters with possibly time-frequency concentrated response. Under certain conditions they can be implemented by using an IFFT followed by low–rate sub–channel filtering. These schemes are referred to as filtered multitone (FMT) modulated systems [1]. If the sub–channels have disjoint frequency response, i.e., they do not overlap in frequency, it is possible to avoid the inter–carrier interference (ICI) and get low inter–symbol interference (ISI) that can be corrected with simplified sub–channel equalization [2]. FMT modulation has the potentiality of achieving better spectral efficiency than OFDM [3].

It is well know that acquisition of the frame (symbol) timing, and carrier frequency in OFDM must be performed very accurately, otherwise a loss in orthogonality between the sub–channels is introduced which translates into ICI [4]. The problem is well understood and several robust techniques are presented in literature, e.g. [5], [6].

In an FMT system the symbol timing and carrier frequency acquisition is still of great importance [7]. In this paper we start reporting the results of the analysis of the effect on performance of the time and frequency misalignments in an FMT system. We investigate different approaches for the estimation of the symbol timing and carrier frequency. The use of training preambles at the beginning of the transmitted frame is commonly used. Its length has to be kept as small as possible especially for burst transmission as in wireless LANs. To this respect, in an OFDM system, synchronization can be acquired, in principle, by exploiting the redundancy of the cyclic prefix [4]. In an FMT system the sub–channel filters inevitably introduce some overhead, i.e. burst transients. However, the overall overhead can be kept small when the training sequence are designed jointly with the sub–channel filters. We propose a completely blind technique for the time-frequency synchronization purpose, that exploits the transmission filter bank characteristics. We report performance curves that confirm our analysis and the efficiency of the proposed synchronization algorithms.

II. Transmitter and receiver model

The scheme that describes a multicarrier system [1] is shown in Fig. 1. The information sequences $a_m(nT), m = 0, 1, ...M-1$ are transmitted in parallel on the M sub–channels. The available transmission bandwidth $B = 1/T_c = K/T$ is subdivided in M sub–channels. If the up-sampling factor K is equal to the number of sub–channels M the system is referred to as critically sampled FMT (CS–FMT), otherwise, when $K = \alpha\, M$, $\alpha > 1$, the system is refered to as non–critically sampled FMT (NCS–FMT). The excess bandwidth factor, $\rho = \alpha - 1$,

[§]This work was supported in part by Italian Ministry of Education, University and Research under the FIRB project: "Reconfigurable platforms for wideband wireless communications", prot. RBNE018RFY.

Proc. of International Symposium on Wireless Personal Multimedia Communications 2003, WPMC 03
Yokosuka, Kanagawa, Japan
October 19-22, 2003
ISSN:1347-6890 © 2003 WPMC Steering Board
Volume 1, pp. 221-225

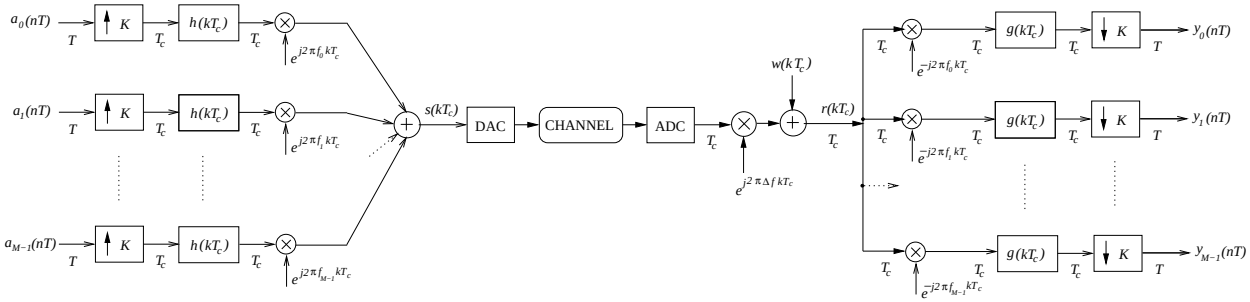

Fig. 1. Transmission block diagram based on filter–bank modulation and demodulation. The i–th, $i = 0, 1, ..., M-1$, sub–channel is carried on the frequency $f_i = B/M = iK/(MT)$. All the sub–channels are filtered with $h(t)$ and $g(t)$, i.e. prototype filter is used.

allows a frequency guard insertion between adjacent sub–channels. In fact in an FMT modulator the transmission prototype filter $h(t)$, that it is assumed identical for every sub–channel, is designed for allowing an ideal frequency separation between adjacent sub-channels. The prototype filter at the receiver $g(t)$ is matched to $h(t)$. The transmission chain include digital–to–analog, and analog–to–digital converters (DAC/ADC). We consider a multipath radio channel with an exponential power delay profile. The system performance is simulated for different values of the root–mean–square time delay spread τ_{rms}. In this paper we have implemented the FMT modulator and the channel model as described in [3] where a detailed description of the system parameters can be found. The main system parameters are: $M = 128$, $\alpha = 1.125$, $B = 25M$Hz, $\tau_{rms} = 40 \div 100n$s, and $SNR = 25$dB. The filters $h(t)$ have support $t \in \{0, T_c, ..., (\gamma M - 1)T_c)\}$, with $\gamma = 12$. The demodulator prototype filter is $g(kT_c) = h^*((\gamma M - k)T_c)$, $\forall k$. In the simulations that follow we deploy square root raseid cosine prototype pulses in NCS–FMT, while in CS- FMT we deploy rectangular windowed pulses see, [3] for details.

III. Timing-Frequency misalignment effects

The modulated signal $s(kT_c)$ (Fig.1) reads

$$s(kT_c) = \sum_{m=0}^{M-1} \sum_{n=-\infty}^{\infty} a_m(nT) h(kT_c - nT) e^{j\,2\pi m \frac{k}{M}} \quad (1)$$

The demodulator output for the sub–channel i at time nT is given by

$$y_i(nT) = \sum_{k=-\infty}^{\infty} r(kT_c) e^{-j\,2\pi i \frac{k}{M}} g(nT - kT_c) \quad (2)$$

where $r(kT_c)$ is the received signal, that we consider impaired by time and frequency offsets,

$$r(kT_c) = s(kT_c + \Delta t)\, e^{-j\,2\pi \Delta f k T_c} \quad (3)$$

for ease of notation an ideal propagation media is assumed. Note also that all subcarriers have the same frequency shift. The timing offset $\Delta t = \varepsilon_t T_c$ is an integer number ε_t of the chip period T_c. The frequency offset $\Delta f = \varepsilon_f / T = \varepsilon_f B/K$ is measured whit respect to the sub–channel bandwidth. Using (1) and (3) in (2), the per-subcarrier output reads

$$y_i(nT) = e^{-j\,2\pi \Delta f \Delta t} \sum_{m=0}^{M-1} \sum_{n'=-\infty}^{\infty} a_m(n'T) e^{j\,2\pi m \frac{\varepsilon_t}{M}} \times \sum_{k=-\infty}^{\infty} h((k+\varepsilon_t)T_c - n'T) g(nT - kT_c) e^{j\,2\pi (m - i - \frac{\varepsilon_f}{\alpha}) \frac{k}{M}} \quad (4)$$

The joint contribution of the timing and frequency offset gives a common phase error $\theta = \exp(-j\,2\pi \Delta f \Delta t)$.

In the following, we separately consider the effects of timing and frequency offsets. For OFDM this effects are well understood [4]. Note that we refer to the discrete time implementation of the OFDM modulator as discrete multitone (DMT) modulator.

A. Timing Offset Effects

Let $\Delta_f = 0$, eq. (4) becomes

$$y_i(nT) = e^{j\,2\pi i \frac{\varepsilon_t}{M}} \sum_{n'=-\infty}^{\infty} a_i(n'T) \times \sum_{k=-\infty}^{\infty} h((k+\varepsilon_t)T_c - n'T) g(nT - kT_c) \quad (5)$$

We observe a signal constellation rotation $\phi = \exp(j\,2\pi i \varepsilon_t / M)$ that it is function of the sub–channel i and of the timing offset error. An ISI contribution appears too. No ICI terms are present, this is due to the spectral containment proprieties of the transmission prototype filters .

B. Frequency Offset Effects

Let $\Delta_t = 0$, eq. (4) becomes

$$y_i(nT) = \sum_{m=0}^{M-1} \sum_{n'=-\infty}^{\infty} a_m(n'T) e^{j\,2\pi \alpha (m-i) n'} e^{-j\,2\pi \Delta f n' T} \times \sum_{p=-\infty}^{\infty} h(pT_c) g(nT - n'T - pT_c) e^{j\,2\pi (m-i) \frac{p}{M}} e^{-j\,2\pi \Delta f p T_c} \quad (6)$$

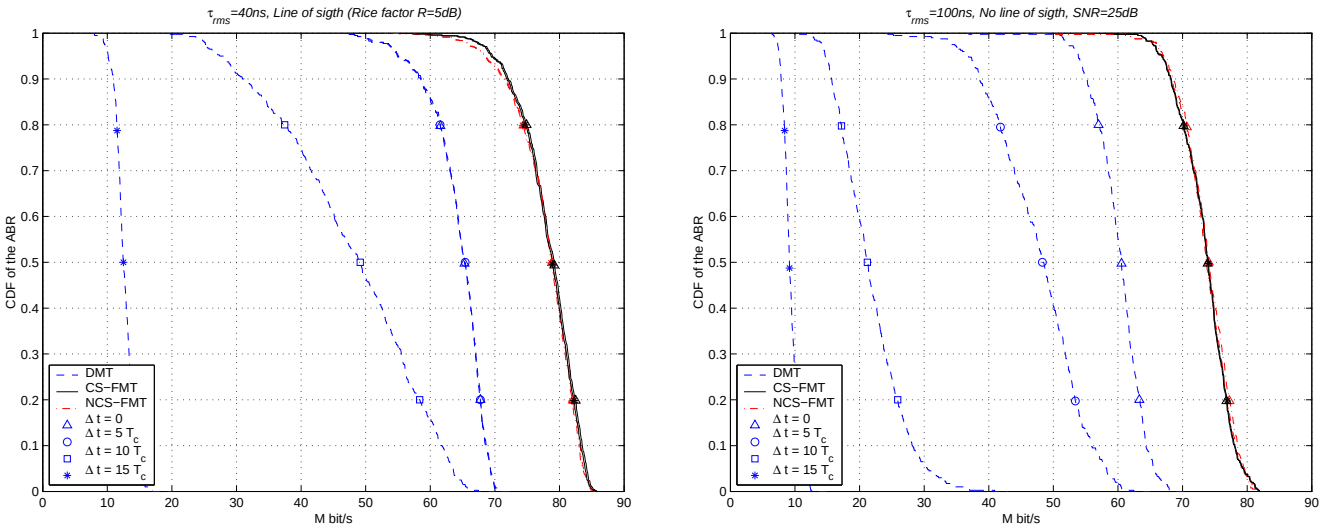

Fig. 2. Complementary distribution function (CDF) of the achievable bit rate (ABR) for DMT, CS-FMT, and NCS-FMT for different timing offsets Δt and different signal propagation conditions.

In this case both ISI and ICI arise. In particular, for $m = i$, i.e., we look at the ISI contribution, a phase rotation of the constellation $\varphi = \exp(-j\,2\pi\Delta f n' T)$ appears. If we evaluate (6) in the frequency domain, it is clear that ICI on the subcarrier i is generated by only one adjacent subcarrier. For example, if Δf is positive and smaller than the subcarriers spacing, the ICI on subcarrier i is due to the subcarrier $i-1$ (assuming band–limited sub–channels). Note that NCS-FMT is more robust to the frequency offset than CS-FMT thanks to the excess bandwidth factor $\rho > 0$.

If we consider a dispersive radio channel, the effects that we have described remain basically the same. It has to be said however, that the radio channel may increase the ISI contribution. A per–subcarrier equalizer is deployed to reduce the ISI impact [2]. Channel estimation that includes also the phase rotations θ, ϕ, and φ is needed for the robustness of the system.

In order to confirm the above analysis we show simulation results in Fig.2. We report the complementary distribution function (CDF) of the achievable bit rate (ABR) [1] for CS-FMT and NCS-FMT in the presence of timing offset. A fractionally spaced decision feedback equalizer (FS–DFE) per sub-channel is used for the system equalization [2]. For comparison purposes we have included the performance of DMT too. In DMT, when Δt plus the channel length, exceed the cyclic prefix, ISI and ICI appear with a conventional one tap DMT equalizer. System performance in the presence of frequency offset is reported in Fig.4 [3]. The simulation confirms the robustness of the FMT system for small values of Δf with respect to DMT. In particular NCS-FMT is more robust than CS-FMT. Generally, FMT achieves higher theoretical transmission bit rates than DMT also in the presence of time and frequency impairments. We point out that the advantages of FMT over DMT is obtained at the expense of some increased receiver complexity. However, several simplified equalization approaches can be adopted [2], [7].

In the following we discuss how to achieve time-frequency synchronization in FMT modulation based transmission systems.

IV. Synchronization strategies

In the following we described two different approaches for time-frequency synchronization of FMT modulated systems. The first one exploits the FMT modulator characteristics allowing for blind time-frequency synchronization. The second one makes use of special multicarrier training symbols.

A. Blind Time-Frequency synchronization

The purpose, herein, is to determine the transmission starting point. The filter bank structure in an FMT modulator introduces memory between successive transmitted symbols that allows for a blind synchronization algorithm. From Fig.1 we observe that each data stream $a_m(\cdot)$ is passed through a prototype interpolator filter with up–sampling factor equal to K. Let $a_m(0)$ be the first data symbol transmitted on sub-channel m. Then, since the prototype filter is real, even, casual and it decays with time, the output samples that correspond to the first half of the filtering transient, have the highest contribution due to the data symbol $a_m(0)$. The remaining contribution is due to the post–cursors data. When $a_m(0)$ is in the correspondence to the filter main taps the interference due to the post–cursor can be neglected. The same properties hold when all filter outputs are summed together and are passed to a common propagation media. We exploit this FMT peculiarity to determine the transmission starting time. This is done in the time–domain before the FMT

demodulator as we show in the following two subsections.

1) Time Correlation: the correlation of the received sequence of samples, that corresponds to two adjacent multicarrier symbols, can be evaluated using the following metric:

$$P(d) = \sum_{\ell=0}^{L-1} r^*((d+\ell)T_c) r((d+M+\ell)T_c) \qquad (7)$$

where $L \leq M$. L is chosen taking into account the delay introduced by the DAC/ADC filters and the radio channel. For the scenario described in this paper, a good choice is $L = M - \gamma - 1$.
Let,

$$R(d) = \sum_{\ell=0}^{L-1} |r((d+\ell)T_c)|^2 \qquad (8)$$

be the received signal energy that corresponds to the first multicarrier symbol. Then, we can define the following synchronization metric:

$$M(d) = \frac{|P(d)|^2}{R^2(d)} \qquad (9)$$

In Fig.3 an example of this metric behavior is shown. Similar plots can be obtained for both CS–FMT and NCS–FMT. A peak in $M(d)$ denotes the start of transmission. The point

$$d_s = \text{argmax}_d M(d) \qquad (10)$$

is in correspondence of the first half of the prototype filter transient.

The correct frame starting point that corresponds to the first useful received sample (in Fig.3 is equal to zero), can can be exactly determined from d_s as a function of the particular prototype filter shape adopted at the transmitter side.

This method is similar to the technique used in DMT [6], but in this case special training symbols are not required.

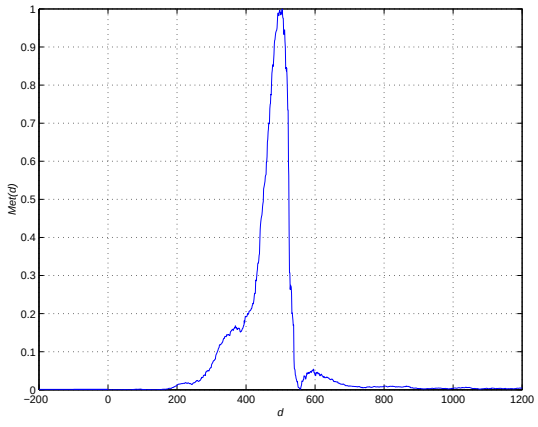

Fig. 3. Example of synchronization metric $M(d)$ for an AWGN channel, SNR=25dB.

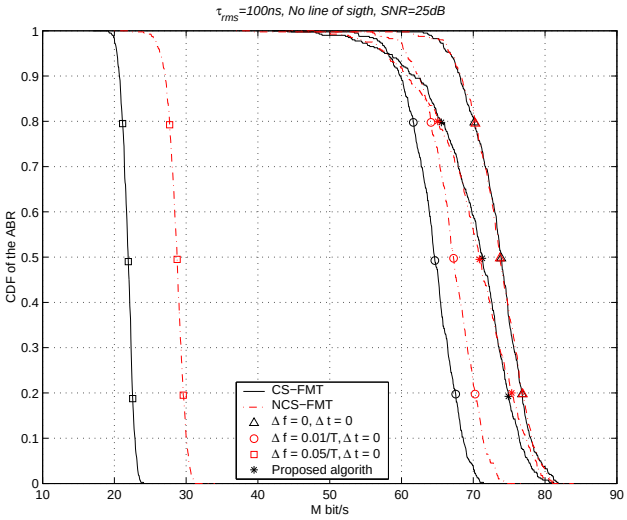

Fig. 4. Complementary distribution function (CDF) of the achievable bit rate (ABR) for CS-FMT, and NCS-FMT for different frequency offset Δf and when joint time-frequency synchronization is obtained with the proposed blind technique for $\Delta f = 0.5/T$.

As shown in Fig.3, the metric $M(d)$ presents an uncertainty around the optimum sampling time. We can average the metric over a window of length L_1 ($L_1 = M/8$ in this paper) to reduce this effect, thus obtaining the metric [8]:

$$M_1(d) = \frac{1}{L_1+1} \sum_{\ell=-L1}^{0} M(d+\ell) \qquad (11)$$

After time synchronization, we can estimate the frequency offset using (7). In fact the main phase difference between two adjacent multicarrier symbols is due to the frequency offset. The metric $P(d)$ accumulates the phase variation, and Δf can be estimated as:

$$\Delta f = \frac{\text{phase}(P(d_s))}{2\pi T/\alpha} \qquad (12)$$

This algorithm allows for the estimation of Δf if it is lower than the subcarriers separation B/M.

Simulation results of the joint time-frequency synchronization are reported in Fig.4 assuming a time dispersive channel, asynchronous transmission and a frequency offset $\Delta f = 0.5/T$. It should be noted that the performance with practical estimation is better than the case when $\Delta f = 0.01/T$ remains uncorrected, and timing is perfect.

2) Energy Level: a simpler time synchronization technique can be obtained by measuring the received energy level. As shown in Fig.5, the energy quantity $R(d)$ in (8) rapidly increases at the beginning of the frame (assuming no previous transmissions). A similar technique has been proposed in [9] for DMT modulation, where power drops are generated by additional null symbols.

Improved estimation can be obtained by the concatenation of the energy level approach followed by the correlation approach of the previous subsection.

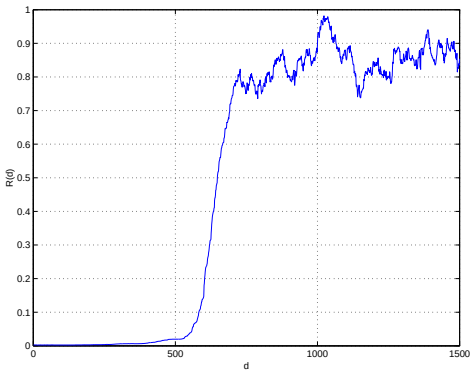

Fig. 5. Example of received signal power $R(d)$ behavior before the demodulator

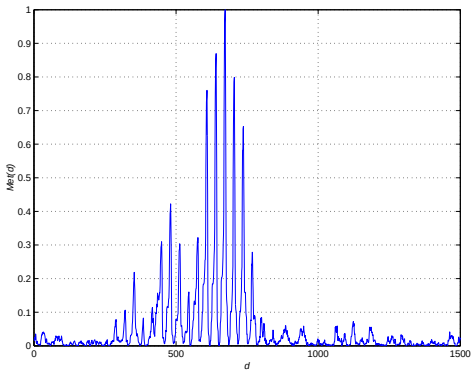

Fig. 6. Example of synchronization metric for an AWGN channel (SNR=25dB) when a burst preamble of the type proposed in [8] has been transmitted.

B. Time-Frequency synchronization using special training symbols

It is very common in DMT systems to insert special preambles at the beginning of the frame for synchronization purposes [6], [8]. The application of this technique to FMT modulation is not straightforward. As an example, we extend to CS-FMT the approach by Schmidl and Cox [6]. That is based on the idea of receiving two identical samples, rotated by a constant phase offset if a frequency offset is present, every period of length, say, MT_c:

$$r((k+M)T_c = r(kT_c)e^{j\,2\pi\Delta f\,MT_c} \qquad (13)$$

Then, the timing and carrier frequency estimation metrics are the ones described in [6]. The problem with FMT is that the prototype filter introduces memory and transients. Therefore, to obtain the desired cyclic property in the received samples a longer preamble has to be used. Let N_p be the length in multiples of T of the equivalent filter that comprises the prototype filter, the DAC/ADC, and the dispersive channel. Then, the received samples corresponding to two adjacent multicarrier symbols, have the cyclic property, after a transient, if we feed each transmit prototype filter with $N_p + 1$ identical data symbols. Different sub-channels may use different data symbols. The drawback with this approach is that the amount of redundancy is a function of the prototype pulse length, and therefore can be significantly high. However, we have found that the preamble length can be significantly shortened by taking into account the fact that the number of significant taps, i.e., the highest energy taps, in the equivalent filter chain is small.

As another example, we report in Fig.6 the synchronization metric when a preamble of the type proposed in [8] is used for the CS-FMT system. Note that the memory introduced by the transmission prototype filter generates a series of peaks in $M(d)$, which translates into some unreliability in the choice of the optimum sampling time.

V. Conclusion

Time-frequency synchronization of filtered multitone (FMT) modulated transmission systems has been discussed. The signal analysis has demonstrated that a time offset is well tolerated in an FMT system when a per–subchannel equalizer is used for ISI cancellation. The frequency offset has a more important impact on the performance due to the ICI contribution.

Various techniques for joint time-frequency synchronization have been examined. Both blind and preamble based approaches have been considered. The blind proposed algorithm has shown good time-frequency offset correction capability with the advantage that no training sequences are required. The comparison between FMT and DMT reveals that the former has higher spectral efficiency. An important open issue remains the estimation of the subcarrier impulse response. To this respect the non–blind methods can allow for easier channel estimation.

References

[1] G. Cherubini, E. Eleftheriou, and S. Ölçer, "Filtered Multitone Modulation for Very High–Speed Digital Subscriber Lines", *IEEE Journal on Sel. Areas in Commun.*, vol.20, NO. 5, pp.1016–1028, June 2002.

[2] N. Benvenuto, S. Tomasin, and L. Tomba, "Equalization Methods in OFDM and FMT Systems for Broadband Wireless Communications", *IEEE Trans. Comm.*, vol.50, NO. 9, pp.1413–1418, Sept. 2002.

[3] A. Assalini, S. Pupolin, and L. Tomba, "DMT and FMT Systems for Wireless Applications: Performance Comparison in the Presence of Frequency Offset and Phase Noise", *In Proc. WPMC'03*, Yokosuka, Kanagawa, Japan, Oct. 19–22, 2003.

[4] R. van Nee and R. Prasad, "*OFDM for wireless multimedia communications*", Artech House Publisher, Boston–London, 2000.

[5] P. H. Moose, "A Technique for Orthogonal Frequency Division Multiplexing Frequency Offset Correction", *IEEE Trans. Comm.*, vol.42, NO.10, pp.2908–2914, Oct. 1994.

[6] T. M. Schmidl and D. C. Cox, "Robust Frequency and Timing Synchronization for OFDM", *IEEE Trans. Comm.*, vol.45, NO.12, pp.1613–1621, Dec. 1997.

[7] A. M. Tonello, "Asynchronous multicarrier multiple access: optimal and sub–optimal detection and decoding", *Bell Labs Technical Journal*, vol.7, NO.3, pp.191–217, 2003.

[8] H. Minn, M. Zeng, and V. K. Bhargava, "On Timing Offset Estimation for OFDM Systems", *IEEE Communications Letters*, vol.7, NO.5, pp.239–241, May 2003.

[9] H. Nogami and T. Nagashima, "A Frequency and Timing Period Acquisition Technique for OFDM Systems", *IEICE Trans. Comm.*, vol.E79-B, NO.8, pp.1135–1146, Aug. 1996.